SEISMIC BEHAVIOR OF SQUARE CONCRETE BEAM-COLUMNS WITH CIRCULARLY DISTRIBUTED ULTRA-HIGH-STRENGTH REBARS

C. Wei [(1)], Y. Sun [(2)], T. Takeuchi [(3)], Y. Takeda [(4)]

[(1)] *Ph.D. Student, Graduate School of Engineering, Kobe University, chuxuan.wei@bath.edu*
[(2)] *Professor, Graduate School of Engineering, Kobe University, sun@person.kobe-u.ac.jp*
China-Japan Resilient and Sustainable Concrete Structures Research Center, Southwest Jiaotong University, China
[(3)] *Assistant Professor, Graduate School of Engineering, Kobe University, takeuchi_t@person.kobe-u.ac.jp*
[(4)] *Toyota T&S Construction, Co. Ltd, takeda2367@toyota-ts.co.jp*

Abstract

One of the authors has proposed a novel method to simply make drift-hardening concrete columns and beam-columns that are intended to be used in concrete structures located in strong earthquake-prone regions just by replacing normal-strength longitudinal rebar with ultra-high yield strength and low bond strength bar (referred to as SBPDN bar). It has been experimentally verified that the use of SBPDN bars (with specific yield strength of 1275 MPa) as longitudinal rebar can provide concrete columns, square and circular, significant drift-hardening capability until the drift level of at least 4.0%. Meanwhile, it has also been found that splitting failure is apt to occur around the contra-flexure section of square beam-columns reinforced by SBPDN bars at the drift level of 2.0% due to the stress concentration in the couplers connecting the SBPDN bars.

This paper proposed new joint methods for SBPDN rebars near the contra-flexure section of square beam-columns, aiming at avoiding the splitting failure and enhancing drift-hardening capability of them. The proposed methods are, (1) circular distribution of longitudinal SBPDN rebars to reduce the damage of concrete around the coupler caused by the stress concentration of each rebar, and (2) utilization of lap joint for SBPDN rebar near the contra-flexure portion.

To verify effectiveness of the proposed methods, four square beam-columns were made and tested under reversed cyclic lateral loading while subjected to constant axial load. The longitudinal rebars in each specimen consisted of eight 12.6 mm SBPDN rebars circularly and uniformly distributed in column section with a minimum distance of 35 mm away from boundary. Main experimental variables were the joint detailing at near the contra-flexure section and the anchorage detailing at both ends of each SBPDN rebar. All specimens had identical geometry; 300 mm square in section and 1020 mm in height to give a shear span ratio of 1.7. The designed concrete strength was 30 MPa, and the axial load ratio was 0.15 for all specimens.

It has been found that circular distribution of longitudinal SBPDN rebar could effectively avoid the splitting failure and enhance drift-hardening capability of square beam-columns up to about 5.0% drift when each SBPDN rebar was connected by conventional coupler near the contra-flexure section. Test results have further indicated that the lap joint of circularly distributed SBPDN rebars near the contra-flexure section would upgrade drift-hardening capability up to 5.0% drift if each SBPDN rebar was screwed along the splice length of 20d, where d expressed the nominal diameter of SBPDN rebar. However, test result did indicate that each SBPDN rebars should be anchored to ring-shape steel plates via nuts at both ends to prevent slippage of SBPDN rebars at large drift, which tended to degrade the lateral resistance of the beam-columns.

Keywords: SBPDN rebars; drift-hardening capability; beam-column; lap connection; ring-shape steel plate fixation.

1. Introduction

Ductile concrete structures had been concerned as the favorite seismic resistance solution in the last decades, but after mega-earthquake such as the Great Sichuan Earthquake (May the 12th of 2008) and Great East Japan Earthquake (March the 11th of 2011), these ductile concrete buildings had to be demolished due to their large residual deformation even they did not collapse after major earthquake, and demolition and replacement of these buildings often requires huge resources. To reduce the cost of recovery and reconstruction, and to make sure the buildings and infrastructures maintains sufficient resistance to intense aftershocks after a major earthquake, the use of high strength materials for reinforced concrete (RC) structures is an available method.

One of the authors has proposed a novel method to simply replace normal-strength longitudinal rebar with the ultra-high yield strength low bond strength rebars (with specific yield strength of 1275 MPa, hereafter referred to as SBPDN rebars). It has been experimentally verified that the use of SBPDN as longitudinal rebar can provide concrete columns, square and circular, positive secondary stiffness, in other words, can keep increasing lateral resistance force of RC columns until large drift ratio (named as drift-hardening capability). Meanwhile, it has also been found that the utilization of SBPDN rebars can control the residual deformation of concrete columns under 15% of the experienced peak deformation [1]. However, due to the low bond strength of SBPDN rebars, it is necessary to be fixed by ring-shape steel plate at both ends. As for RC columns under double curvature deformation, to guarantee their drift-hardening capability, the SBPDN rebars should not only be fixed by ring-shape steel plate at both ends, but should be securely fixed near contra-flexure section as well. However, previous research indicated that splitting failure is apt to occur around the contra-flexure section of square beam-columns reinforced by SBPDN rebars at the drift level of 2.0% due to the stress concentration in the couplers connecting the SBPDN rebars [2].

This paper proposed new joint methods for SBPDN rebars near the contra-flexure section of square beam-columns, aiming at avoiding the splitting failure and enhancing drift-hardening capability of them. The proposed methods are, (1) circular distribution of longitudinal SBPDN rebars to reduce the damage of concrete around the coupler caused by the stress concentration of each rebar, and (2) utilization of the lap joint of SBPDN rebars near the contra-flexure section with each rebar screwed along the splice length of 20d, where d expressed the nominal diameter of SBPDN rebar, which can simplify construction process and provide sufficient drift-hardening capability. To verify the effect of the proposed methods, four square beam-columns were fabricated and tested under reversed cyclic lateral loading while subjected to constant axial load. Accompanying with the experiments, an analytical method that can take effect of slippage of longitudinal rebars into consideration was also presented. Since validity and accuracy of the proposed method had been verified [1], the effect of the new joint methods will be proved by comparing the analytical results with the tested ones.

2. Experimental program

2.1 Details of specimens

To achieve the aforementioned goals, four one-third scale RC columns were fabricated and tested under reversed cyclic lateral loading while subjected to constant axial load. Fig. 1 shows the reinforcements and section details of tested specimens, while Table 1 indicates the outlines and the main tested results of all tested columns.

All specimens had identical geometry, 300 mm square in section and 1020 mm in height to give a shear span ratio of 1.7 for columns under double curvature deformation. The designed concrete strength was 30 MPa, and the axial load ratio n was 0.15 for all specimens, ready mixed concrete made up of Portland cement and aggregates with maximum diameter of 20 mm was utilized to fabricate the specimens. As for reinforcements (mechanical properties shown in Table 2), the longitudinal rebars in each specimen consisted of eight 12.6 mm SBPDN rebars circularly and uniformly distributed in column section with a minimum distance of 35 mm away from boundary. Besides, all columns were laterally confined by D10-SD345 hoops with spacing of 55 mm to prevent the local buckling of longitudinal rebars and to provide shear resistance. To protect the concrete at each corners of section, square D6-SD295A stirrups with spacing of 55 mm was conducted.

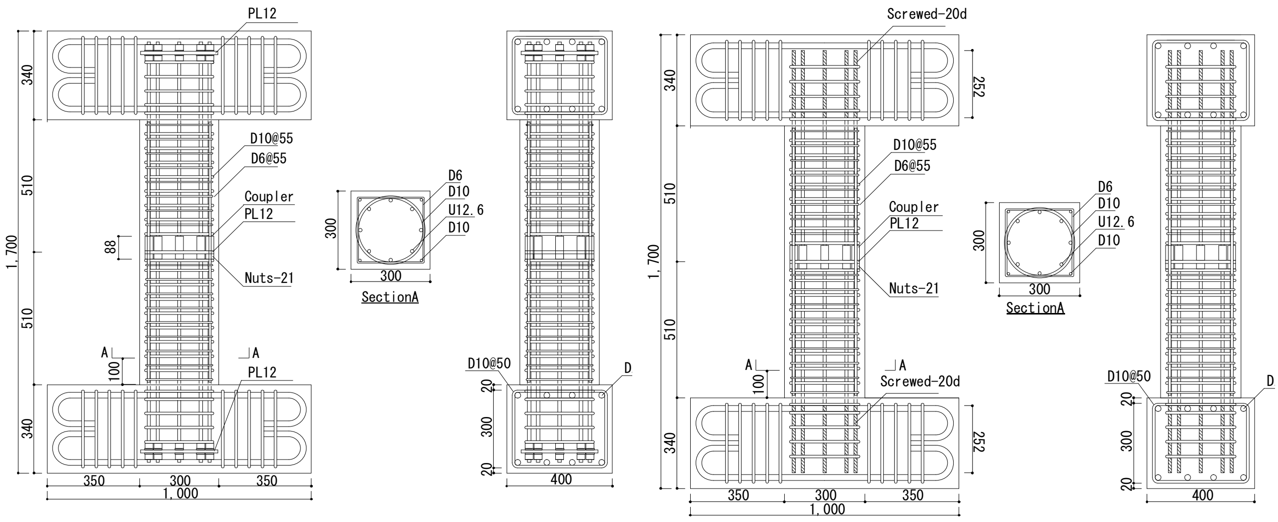

(a) D-P (b) DS-P

(c) D-S (d) DS-S

Fig.1 – Reinforcements and section details of tested columns

Previous research indicated that the bond strength of SBPDN rebar is about 3 MPa when it was embedded in concrete with compression strength of about 40 MPa, which is about one-fifth comparing with ordinary rebar [1]. SBPDN rebars of specimens in previous studies [2] were fixed by ring-shape steel plate via high strength nuts to prevent the slippage between rebars and concrete at both ends. Besides, other previous research also proved that if the SBPDN rebar was screwed its bond strength was increased to 21.8 MPa [3]. Thus, lap joint with screwed SBPDN rebars is a potential fixation method to simplify construction procedure, which makes it possible for RC column reinforced with SBPDN rebars to be applied in precast concrete structure. To verify the effect of the proposed method, main experimental variables were the joint detailing near the contra-flexure section and the anchorage detailing at both ends of each SBPDN rebar, and the details of connection of each specimen are listed in Table 1.

Table 1 – Outlines of the tested specimens and main test results

<table>
<tr><th rowspan="2">Specimen</th><th rowspan="2">a/D</th><th rowspan="2">n</th><th rowspan="2">f'_c (N/mm^2)</th><th colspan="2">Anchorage</th><th colspan="2">Longitudinal rebars</th><th colspan="2">Transverse rebars</th><th rowspan="2">Q_{exp} (kN)</th></tr>
<tr><th>Contra-flexure section</th><th>Beam-column joint</th><th>Type</th><th>ρ_s(%)</th><th>Type</th><th>ρ_h (%)</th></tr>
<tr><td>D-P</td><td rowspan="4">1.7</td><td rowspan="4">0.15</td><td>46.7</td><td>ring-shape steel plates</td><td rowspan="2">ring-shape steel plates</td><td>8-U12.6 ①</td><td rowspan="4">1.11</td><td rowspan="4">D10 @55</td><td rowspan="4">2.36</td><td>319.2</td></tr>
<tr><td>D-S</td><td>44.6</td><td>screwed lap joint</td><td rowspan="3">8-U12.6 ②</td><td>333.0</td></tr>
<tr><td>DS-P</td><td>40.0</td><td>ring-shape steel plates</td><td rowspan="2">screw threads</td><td>278.1</td></tr>
<tr><td>DS-S</td><td>39.4</td><td>screwed lap joint</td><td>266.0</td></tr>
<tr><td colspan="11">a/D: shear span ratio; n: axial load ratio; f'_c: concrete cylinder strength; ρ_s: reinforcement ratio of longitudinal rebars; ρ_h: volumetric ratio of transverse rebars; Q_{exp}: measured ultimate lateral force;</td></tr>
</table>

Table 2 – Mechanical properties of the steels

Type		f_y (N/mm^2)	ε_y (%)	f_u (N/mm^2)	E_s (kN/mm^2)
D6	SD295A	377	0.20	513	192.40
D10	SD345	324	0.19	445	173.82
U12.6①	SBPDN 1275/1240	1361	0.84	1470	211.58
U12.6②	SBPDN 1275/1240	1394	0.84	1467	216.63

f_y: yield stress; f_u: ultimate stress; E_s: Young's modulus; ε_y: yield strain;

2.2 Test setup and loading program

The test setup that was shown in Fig.2 was applied to deform the columns under a double curvature pattern. The cyclic reversals of lateral force were conducted by two horizontal hydraulic jacks with capacities of 300kN in pulling and 500kN in pushing respectively, while a pantograph system was used to guarantee the parallel of top and bottom stub during the deformation of columns. One vertical hydraulic jack with capacity of 1000kN was connected to stiff loading via a roller, which was applied to provide constant axial compression load, the axial and lateral loadings were controlled by two different loading systems.

Fig.4 indicates the locations of displacement transducers (DTs) of tested columns. The lateral displacements of each specimen were measured by two lateral DTs noted as No.1 and No.2, and the average of the displacements measured by them was divided by the height of column to give the drift ratios (R). The lateral loading was controlled by drift ratio of column, west was applied as the initial pushing (plus) direction while east was the initial pulling (minus) direction. As is shown in Fig. 3, the lateral loading was reversed two complete cycles at each level of displacement till drift ratio reached 2%, and one cycle was conducted at each level of displacement after drift ratio became larger than 2%. However, during the test of specimen D-S, the lateral displacement of the column was doubled in the control system of lateral loading by mistake. As a result, only half of the target drift ratios were reached, and the loading history of specimen D-S was different from the other specimens.

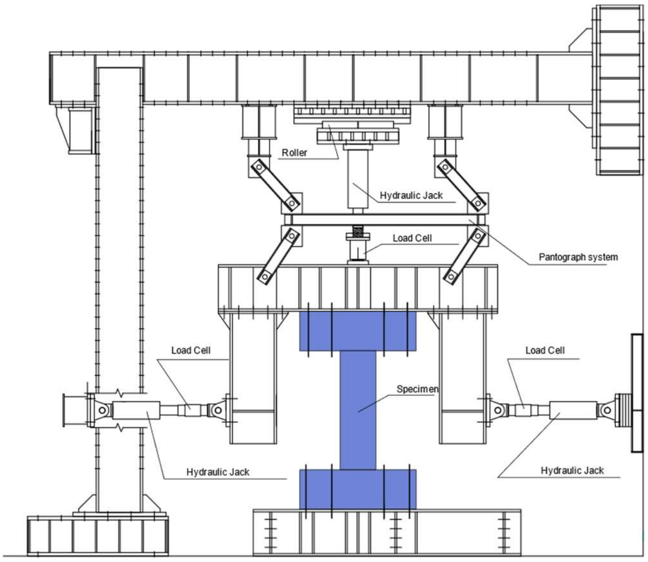

Fig.2 – Test setup for double curvature columns

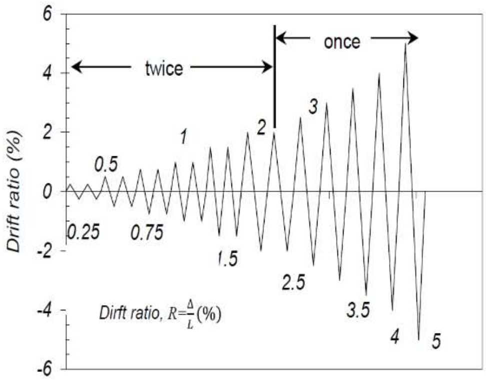

Fig.3 – Loading program

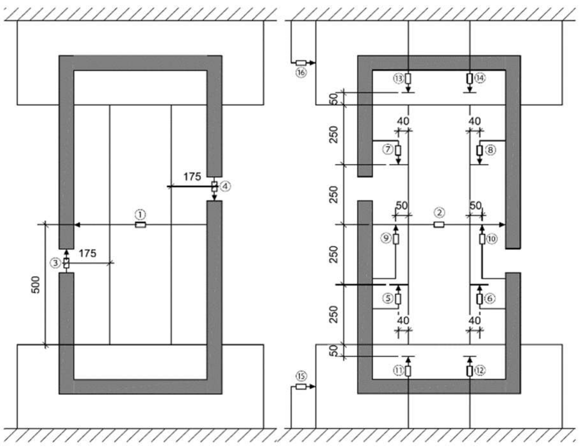
(a) North (b) South

Fig.4 – Location of displacement transducers (DTs)

3. Experimental results and discussions

3.1 Cracks and damages of specimens

Recorded typical events of all specimens were summarized in this section. Fig.5 shows the developments of cracks that were observed from north and east side of each specimen, the grid spacing is 50 mm, red lines and blue lines indicate the cracks that were recorded at the peak of relative plus and minus cycles separately, while the black blocks express the spalling of cover concrete, and because of the abovementioned mistake, cracks of specimen D-S were not recorded when its drift ratio became larger than 3%. As can be seen in Fig.5, most of the damage concentrated in the plastic hinge region (1.0D away from column base, D is the section width of specimen) for all specimens, and only few cracks and slight damage, which can be simply repaired, were observed on the surfaces of tested columns till their drift ratio reached 2.0%. Besides, vertical bond cracks were firstly confirmed when drift ratio reached 2%, located near the middle and corner of specimen DS-P and DS-S, which indicated that the SBPDN rebars of DS group were not completely fixed. Moreover, splitting cracks were not observed around the contra-flexure section of specimen D-P until the drift ratio reached 4%, so circularly distribution of longitudinal rebars can retard the development of splitting failure caused by stress concentration in the coupler that connecting SBPDN rebars.

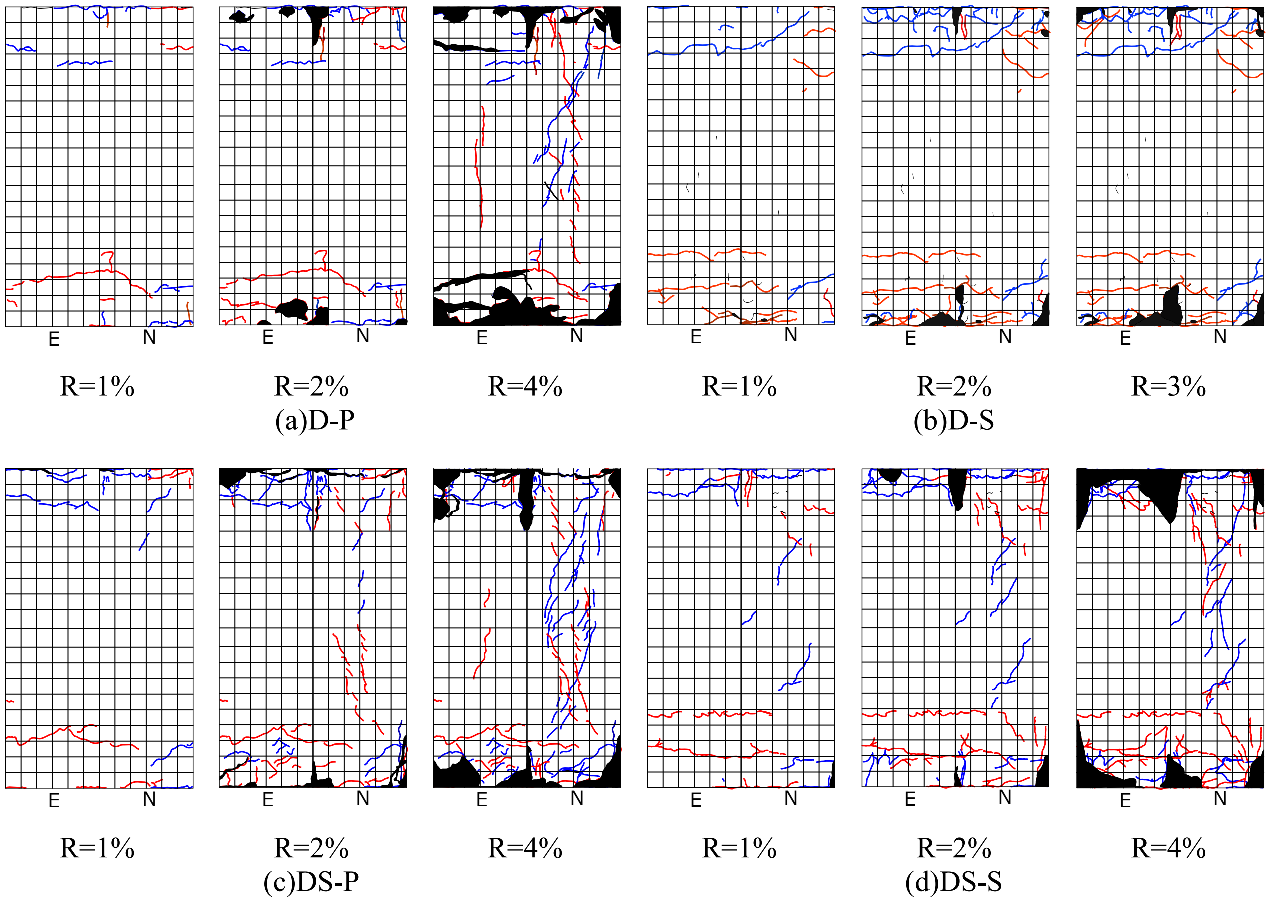

Fig.5 – Cracks and damages observed on specimens

3.2 Hysteretic behaviors

Fig.6 shows the lateral load versus drift ratio relationships of all specimen, while the red dashed line in each graph represents the P-Δ effect of axial compression on the lateral resistance force. The solid diamonds in Fig.6 indicate the tested peak loading, and the measured ultimate strength of each specimen was summarized in Table 1.

As is shown in Fig.6, for the D group of which SBPDN rebars anchored to ring-shape steel plates via nuts in the beam-column joints, obvious drift-hardening behavior was observed even up to large deformation until the drift ratio reached 5%. The lateral resistance force of specimen D-P descend during the cycle of 3.5% because of the slippage between top base of column and the rigid steel frame, and the lateral resistance of D-P raised again after the top base was fixed. As for the push direction of D-P, a slightly decrease of lateral resistance was observed at the drift ratio of 4% due to significant spalling of the cover concrete, but the descent of lateral resistance force along with lateral displacement was much more gently than that caused by P-Δ effect. Although the test of D-S was prematurely terminated at the drift ratio of 3% because of the abovementioned disorder of the DTs to measure the lateral displacement, the lateral resistance force of D-S kept increasing till the drift ratio of 5% during the last loading cycle.

As for the DS group, no significant difference between D group and DS group was observed till the drift ratio of 2%. However, with the P-Δ effect kept increasing and the spalling of cover concrete kept getting severely along with the development of deformation, the lateral resistance forces of DS-P and DS-S decreased from the drift ratio of 2.5% and 2% separately. Therefore, the simple fixation of SBPDN rebars at both end of

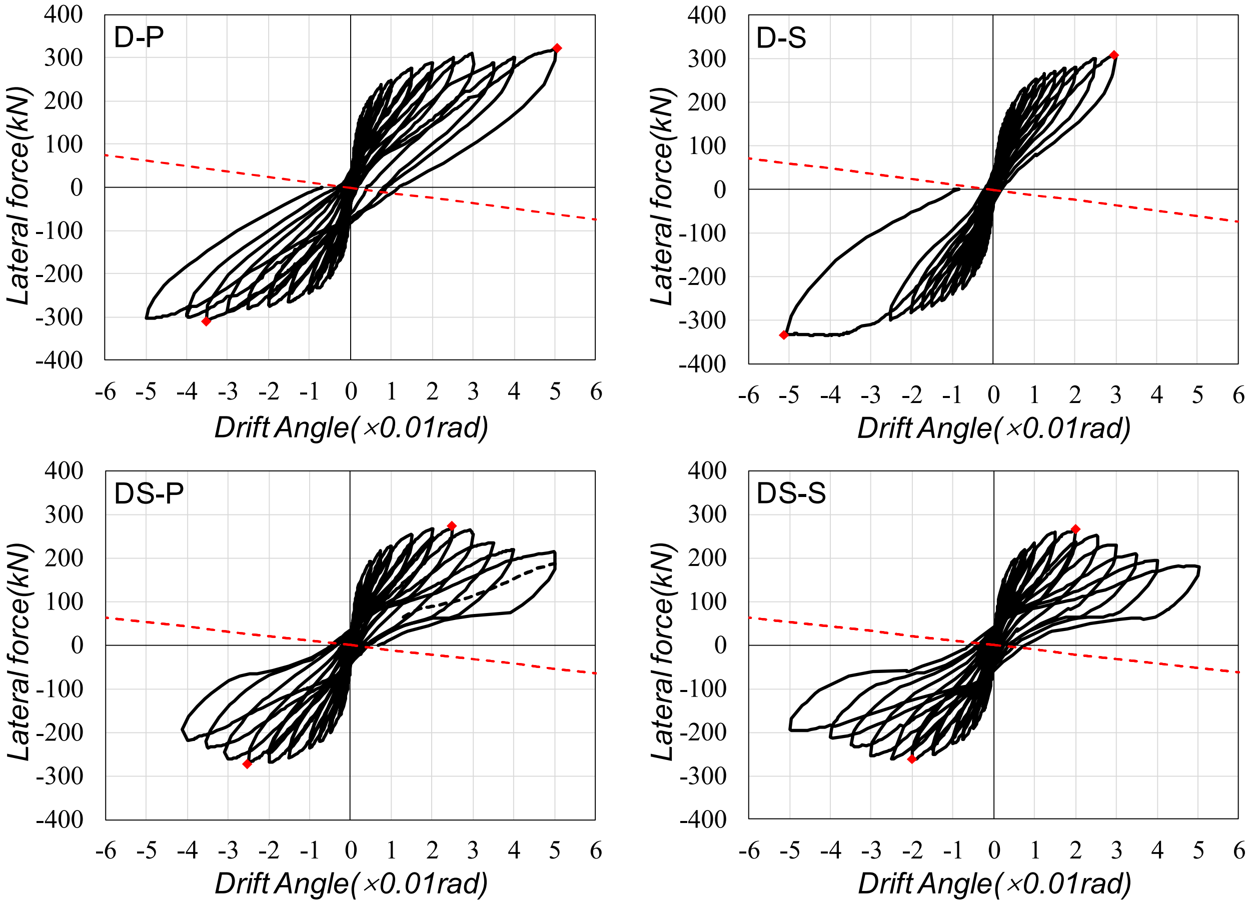

Fig. 6 – Measured hysteretic lateral load versus drift ratio relationships

DS group cannot assure the drift-hardening capability of RC columns, and the reason will be discussed in section 3.3. During the test of specimen DS-P, due to the mistake of operator, the specimen was unloaded immediately and abruptly once its drift ratio reached 5%, the unloading curve was marked by the black dashed line shown in Fig.6

Fig.7 indicates the test results of residual deformation. Due to the slippage between the top base of specimen D-P and the rigid steel frame, significant ascent of drift ratio was observed at the pull direction when drift ratio reached 3%. As for the push direction, it was found that regardless the fixation method of ultra-high strength low bond strength rebars at both end of tested specimens, the use of SBPDN rebars can control the residual drift ratio of RC beam-columns under 15% of the experienced peak drift ratio.

To evaluate the energy dissipation capability of the tested specimens, equivalent viscous damping coefficient h_{eq} proposed by Jacobsen [4] was calculated and summarized in Fig.8. Since specimen D-S experienced more loading cycles due to different loading history, the value for h_{eq} of D-S was relative lower than those of other specimens. Besides, all specimens exhibited stable and nearly constant equivalent viscous damping coefficient varying between the value of 0.05 and 0.1 till drift ratio reached 2.5%, and there was no significant difference among the specimens with different fixation at both ends. Specimen D-P maintained this constant value for h_{eq} till the end of test till drift ratio reached 5%, except the ascent at the drift ratio of 3.5% due to the descent of lateral resistance force caused by the slippage between the top base of specimen D-P and the rigid steel frame. It was also found that the equivalent viscous damping coefficient measured from DS group increased gradually after the drift ratio of 2.5%, accompanying with the degradation of lateral resistance force.

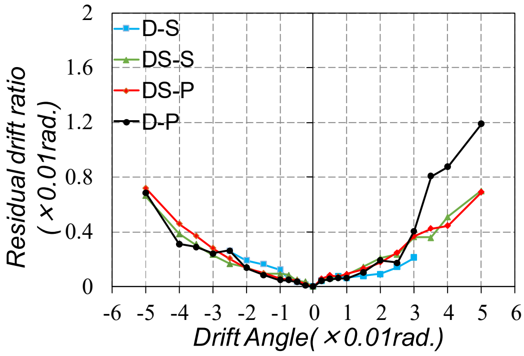

Fig. 7 – Measured residual drift ratio

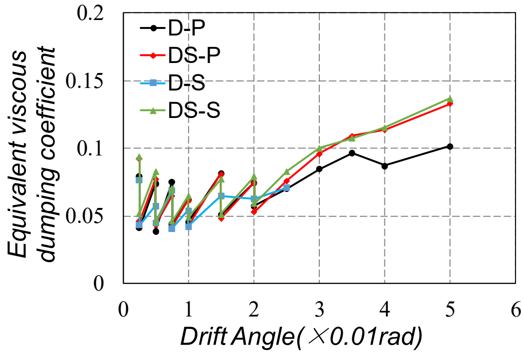

Fig. 8 – Measured equivalent viscous damping coefficient

3.3 Strains of longitudinal rebars

To measure strains in longitudinal rebars, strain gauges were embedded via an adhesive to the surface of rebars located near 35mm away from top and bottom stub of all specimens, available measured data was summarized in Fig.9. the red lines and black lines represent the strain measured from the initially tensile and compression SBPDN rebars respectively. As is shown in Fig.9, the strains of longitudinal rebars in specimen D-P and D-S exhibited stable ascent along with the increasing of deformation till the drift ratio of 3.5%, so the ring-shape steel plates can fix the SBPDN rebars without slippage at column ends. Besides, by comparing the measured results of specimen D-P and D-S, the screwed lap joint can fix longitudinal rebars without slippage at the contra-flexure section. Moreover, due to the low bond strength of SBPDN rebars delayed the yielding of longitudinal rebars in RC columns [5], the strains of longitudinal rebars did not reach its yield strain (0.84%) till the end of test.

As for DS group, the strains of longitudinal rebars in specimen DS-P and DS-S decreased after peak at the drift ratio of 2.5% and 2.0%, respectively, coincided with the decrease of lateral resistance force. This is because the simple fixation by the screw threads of SBPDN rebars at both ends of specimens could not provide sufficient bond strength to sustain the high stress developed in SBPDN bars.

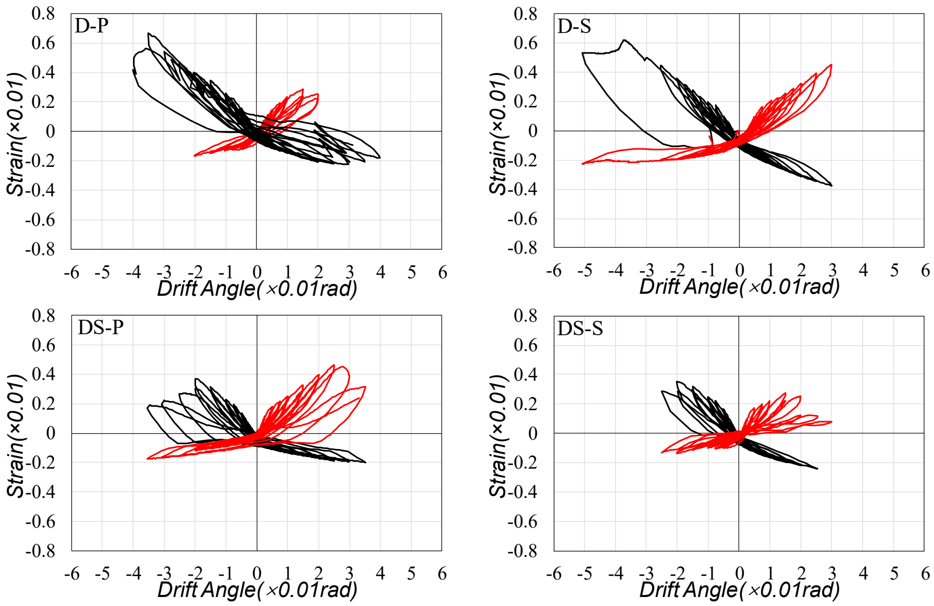

Fig. 9 – Strains of main reinforcements

4. Analytical method for assessing seismic behaviors of the proposed columns

4.1 Assumptions and procedures of analysis

Since the slippage between reinforcement and concrete cannot be measured in this experiment, a new analytical method that can consider the bond-slip characteristic of steel rebars in concrete components, which had been proved that it can reasonably and reliably predict the seismic behaviors of concrete columns reinforced by SBPDN rebars [1], was presented in this section.

To simulate the seismic behavior of concrete columns reinforced by SBPDN rebars, the following assumption are made: 1) concrete only resist compression stress, 2) the concrete plane remains plane after bending and cover conrete do not spall off, 3) the constitutive model of concrete proposed by Sakino and Sun which can take the confinement effect of stirrups into consideration, was applied in this analysis, details can be found in [6], 4) the bond-slip relationship of the SBPDN rebars follows the model proposed by Funato et al [3], and the Menegotto-Pinto model [7] is utilized as the constitutive model of SBPDN rebars, 5) the lateral displacement of column concentrates in the plastic hinge region (1.0D), 6) strain and stress of the longitudinal rebars are uniformly distributed in the plastic hinge region, 7) according to previous research, the maximum bond strength of SBPDN rebar is taken as 3 N/mm^2 for the concrete with compressive strength about 40 N/mm^2 [3], and the longitudinal rebar is completely fixed at both ends without slippage.

The analysis of column section in plastic hinge region is significant in evaluation of hysteresis response of concrete components, a reasonable and reliable finite fiber method [8] was used to conduct the simulation (details of the finite fiber method is shown in Fig.10). To simplify the procedure of analysis, the coloumn was divided into two cantilever columns as is shown in Fig.11. According to the abovementioned basic assumptions and relative models, processes of analysis can be described as follows: (1) As shown in Fig.11, a concrete column can be discreted into hinge region and bond confinement springs (BCS) region, including joint end and free elastic end. (2) Calculate the curvature φ_k of the column in the hinge zone based on the fifth assumption for a given drift ratio R_k. (3) Give an initial value ε_k to the strain at the center of section, and the strain distribution of concrete ε_{ci} across the section depth can be obtained following the second assumption. (4) The distribution of rebar strain which the slip effect has been taken into account can be computed by the iterative procedures, details can be found in [5]. (5) Use the strain obtained above to calculate the concrete stress and the rebar stress according to respective constitutive law. (6) Calculate the internal axial load N and the bending moment M. (7) If the axial load N balances the applied axial load P within a tolerable error, the calculated M is taken as the bending moment M_k corresponding to the given R_k. If not, try a new center strain ε_k, and repeat from step (4). (8) Calculate the lateral force V_k corresponding to R_k which can satisfy static equilibrium. (9) Give a new R_k and repeat the above steps till the target drift ratio.

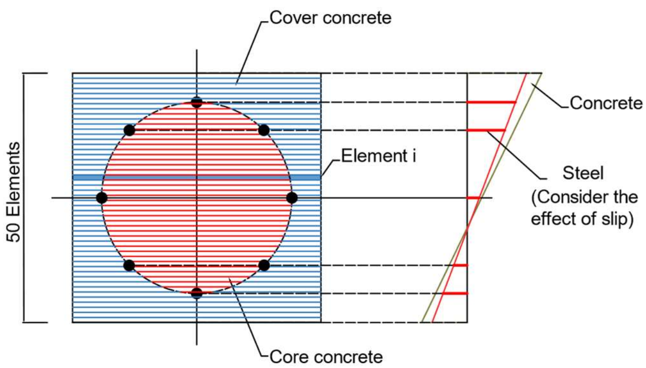

Fig. 10 – Section and strain distribution in column section

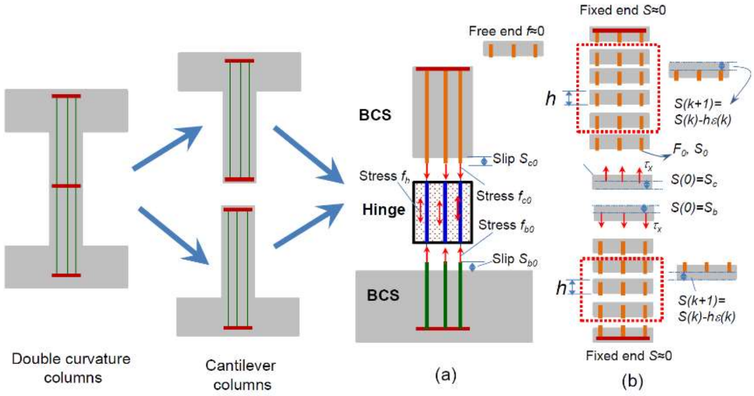

Fig. 11 – Discrete model of concrete member [5]

4.2 Comparison between tested and analytical results

Fig.12 shows comparisons between the experimentally measured hysteresis curves and the theoretical predictions by the presented method for specimen D-P and D-S, and the theoretical hysteresis loops exhibits accurate agreement with the experimental curves with difference of less than 10% on the conservative side. Since the analytical results agree very well with the tested ones with the assumption that SBPDN bars were securely fixed without slippage at their both ends and the contra-flexure section in this simulation, these results support the conclusion that the screwed lap joint can fix the SBPDN rebars at the contra-flexure section of concrete column.

5. Conclusion

This paper proposed new joint methods for SBPDN rebars near the contra-flexure section and colum base of square RC beam-columns, to verify the effectiveness of the proposed methods, four square beam-columns were fabricated and tested under reversed cyclic lateral loading while subjected to constant axial load. Based on the experimental and analytical results summarized in this paper, the following conclusions can be drawn:

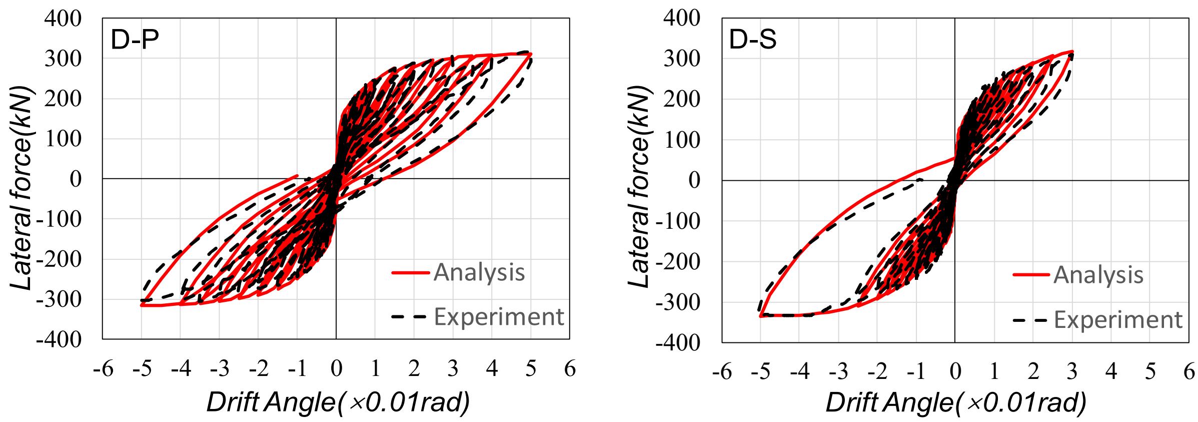

Fig. 12 – Comparisons between tested and analytical Lateral load – drift ratio relationship

(1) Circular distribution of longitudinal SBPDN rebar could effectively reduce the stress concentration in the couppler near the contra-flexure section of column, which can avoid the splitting failure, thus it can guarantee drift-hardening capability of square beam-columns even up to large drift ratio about 5.0%.

(2) The lap joint of circularly distributed SBPDN rebars near the contra-flexure section could provide sufficient drift-hardening capability up to drift ratio of 5.0% if each SBPDN rebar was screwed along the splice length of 20d, where d expressed the nominal diameter of SBPDN rebar.

(3) Test results did indicate that slippage of SBPDN rebars in the beam-column joints at large drift tended to degrade the lateral resistance of the beam-columns, and the screw threads could not fix SBPDN rebarsin the beam-column joints. Further research is necessary to improve the proposed anchorage method, such as increasing the length of the screw threads of SBPDN bars or the development length in the beam-colomn joint.

6. Acknowledgements

The authors wishes to express deepest gratitude to Toyota T&S construction Co. Ltd for their finacial support, and sincere appreciation to Neturen Co. Ltd for the SBPDN rebars they provided.

7. References

[1] Sargsyan G. et al. (2016): SEISMIC BEHAVIOR AND ASSESSMENT OF DRIFT-HARDENING CONCRETE COLUMNS, *16th World Conference on Earthquake*, Santiago, Chile, Paper No. 664

[2] Sun Y. et al. (2013): Seismic Behavior and Performance-Based Design of Resilient Concrete Columns, *Applied Mechanics and Materials*, *Vols. 438-439,* 1453-1460.

[3] Funato Y. et al. (2012): Modeling and application of bond characteristic of high-strength reinforcing bar with spiral grooves, *Proceedings of the Japan Concrete Institute*, 34(2), 157-162, (in Japanese).

[4] Jacobsen LS. (1960): Damping of composite structures, *Proceedings of 2nd world conference on earthquake engineering,* (2):1029-1044.

[5] Sun Y. et al. (2006): Analytical Study of Cyclic Response of Concrete Members Made of High-Strength Materials, *The Eighth U.S. National Conference on Earthquake Engineering*, Paper No. 1581.

[6] Sakino K, Sun Y (1994): Stress-strain curve of high-strength concrete, *Journal of Constr. and Structural Engineering of AIJ*, 466:95-104. [In Japanese]

[7] Sun Y. et al. (2006): Modeling of complete stress-strain relationship for high-strength steels, *The First European Conference on Earthquake and Seismology*, Paper No. 760.

[8] Sun Y., Sakino K., Yoshioka T (1996): Flexural behavior of high-strength RC columns confined by rectilinear reinforcement, Journal of Structural and Construction Engineering, *Architectural Institute of Japan*, No. 486, 95-106.

